Journal of Alloys and Compounds 489 (2010) 566–569

Contents lists available at ScienceDirect

Journal of Alloys and Compounds

journal homepage: www.elsevier.com/locate/jallcom

Low-temperature synthesis and photoluminescence of ZnO nanostructures by a facile hydrothermal process

P.G. Li*, S.L. Wang, W.H. Tang

Department of Physics, Centre for Optoelectronics Materials and Devices, Zhejiang Sci-Tech University, Xiasha College Park, Hangzhou 310018, China

ARTICLE INFO

Article history:
Received 22 August 2009
Received in revised form
13 September 2009
Accepted 17 September 2009
Available online 25 September 2009

Keywords:
Semiconductors
Nanostructured materials
Chemical synthesis
Optical property

ABSTRACT

We reported a facile route to large-scale ZnO nanostructures by a poly (styrene-*alt*-maleic acid sodium) (PSMA)-assisted hydrothermal process. Various nanostructures including nanowires, nanobelts and nanorod arrays were fabricated depending on the experimental conditions. The structural studies reveal that all the nanostructures are single crystal with hexagonal phase and preferentially grow along [0 0 0 1]. The organic additive PSMA offers a spatial template for the one-dimensional (1D) growth of ZnO. The photoluminescence (PL) spectra of these nanostructures exhibit coexistence properties of ultraviolet (UV) and green emission. The nanorod arrays and nanobelts exhibit the strongest UV performance and green emission, respectively. We deduce that quantity of surface defects should be responsible for the difference in PL properties of these nanostructures.

1. Introduction

One-dimensional (1D) nanostructures such as nanowires, nanobelts and nanorods have attracted considerable attentions over past two decades due to their unique physical, optical and electric properties [1–5]. As a direct wide band-gap (3.37 eV) semiconductor with large exciton binding energy (60 mV), ZnO is one of the most important semiconductors for its unique optical and electronic applications in future electronic and photonic devices [6,7]. 1D ZnO nanostructures are among the most promising and extensively studied nanostructures due to their potential optoelectronic applications including light-emitting diodes, laser diodes, photodetectors, solar cells, nanogenerators and nanopiezotronics [8–13]. A number of methods have been used to fabricate ZnO nanowires such as MBE, MOCVD, PLD, thermal evaporation, chemical vapor transport, template-assisted method, solution-phase synthesis, and hydrothermal/solvothermal synthesis [14–21]. Among these synthesis methods, hydrothermal/solvothermal methods are the most efficient to synthesize various nanostructures due to their simple, high yield and low cost. In the hydrothermal/solvothermal process, organic additive-assisted synthesis of ZnO nanostructures is more attractive because these organic additives can induce multi-growth models that further result in various nanostructures. In this paper, we develop a novel hydrothermal route to synthesize ZnO nanostructures assisted by an organic additive poly (styrene-*alt*-maleic acid sodium) (PSMA). ZnO nanowires, nanobelts and nanorod arrays grown on 6H–SiC substrates were fabricated depending on the experimental conditions. Moreover, the growth mechanisms of the nanostructures are proposed and the corresponding photoluminescence (PL) properties are studied.

2. Experimental procedure

2.1. Synthesis of ZnO nanowires and nanobelts

The organic additive poly (styrene-*alt*-maleic acid sodium) (30 wt.% solution in water, typical Mw: 120,000) (PSMA) was purchased from Sigma–Aldrich Inc., and all the chemicals were analytic grade reagents without further purification. Experimental details were listed as follows: 5 ml aqueous solution of $Zn(NO_3)_2{\cdot}6H_2O$ (0.05 M), 2 ml solution of PSMA and 35 ml aqueous solution of Na_2CO_3 (2.5 M) were successively added into 50 ml Telfon-lined stainless steel autoclave. The obtained mixture was stirred for an hour and then the autoclave was sealed and maintained at 160 °C for 24 h. After the reaction was completed, the as-synthesized precipitates were confirmed as ZnO nanowires. By the similar experimental procedure, 5 ml aqueous solution of $Zn(NO_3)_2{\cdot}6H_2O$ (0.05 M), 4 ml solution of PSMA and 35 ml aqueous solution of Na_2CO_3 (2.5 M) were mixed together, and the chemical reaction was conducted at the similar experimental condition. The final product was identified as ZnO nanobelts.

2.2. Synthesis of ZnO nanorod arrays on 6H–SiC substrates

Well-aligned ZnO nanowire arrays on 6H–SiC substrates were synthesized by two-step growth process. First, ZnO seeding layer was grown on the 6H–SiC substrates by a facile sol–gel method reported from the literatures [22,23]. Then, 5 ml aqueous solution of $Zn(NO_3)_2{\cdot}6H_2O$ (0.05 M) and 35 ml aqueous solution of Na_2CO_3 (2 M) were successively added into 50 ml Telfon-lined stainless steel autoclave and stirring for an hour. Finally, ZnO seeding layer-coated 6H–SiC substrates were put into the mixed solution and the maintained at 150 °C for 24 h in the sealed Telfon-lined stainless steel autoclave. Finally the autoclaves was cooled to room

* Corresponding author. Tel.: +86 571 86843468; fax: +86 571 86843222.
E-mail address: peigangiphy@yahoo.com.cn (P.G. Li).

0925-8388/$ – see front matter © 2009 Elsevier B.V. All rights reserved.
doi:10.1016/j.jallcom.2009.09.110

temperature, the 6H–SiC substrates were then washed with distilled water for several times, and the as-deposited product was identified as ZnO nanorod arrays.

2.3. Characterization

Powder X-ray diffraction (XRD) data used for structural analysis was collected on rotating-anode rigaku Pint-2400 X-ray diffractometer with Cu Kα radiation. The diffraction peaks was indexed according to the standard diffraction data shown in the software PCPDFWIN (http://icdd.com/products/pdf2.htm). The crystal lattice constants were calculated by using the computer software Dicyol [24]. We add the content in the characterization section. The morphologies of the as-synthesized ZnO were examined by field-emission scanning electron microscope (FEI XL30 S-FEG). The transition electronic microscopy (TEM) images and high-resolution TEM (HRTEM) of samples were collected on the JEOL 2010F transmission electron microscope equipped with energy-dispersive X-ray spectroscopy (EDS). Photoluminescence (PL) spectra of the products were carried out at RT using the 325 nm line of a He–Cd laser with an output power of about 2 mW as the excitation source.

3. Results and discussion

Fig. 1a shows a typical XRD pattern of the as-synthesized ZnO nanowires. All the diffraction peaks can be indexed to wurtzite ZnO with lattice constants of $a = 3.251$ Å and $c = 5.212$ Å, agreeing well with the calculated diffraction pattern (JSPDS No. 36–1451). No other diffraction peaks are detected within the instrumental resolution, indicating that the products are ZnO with high purity. Fig. 2a gives an overview of the products, revealing well-defined nanowires formation of the products. These nanowires are of uniform size, smooth surface and good toughness, as shown in the

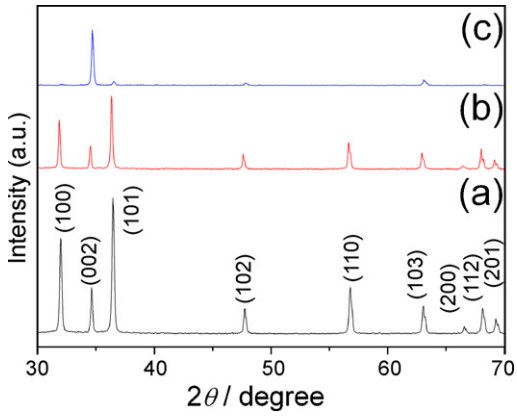

Fig. 1. XRD patterns of the obtained ZnO nanostructures: (a) nanowires; (b) nanobelts; (c) nanorod arrays.

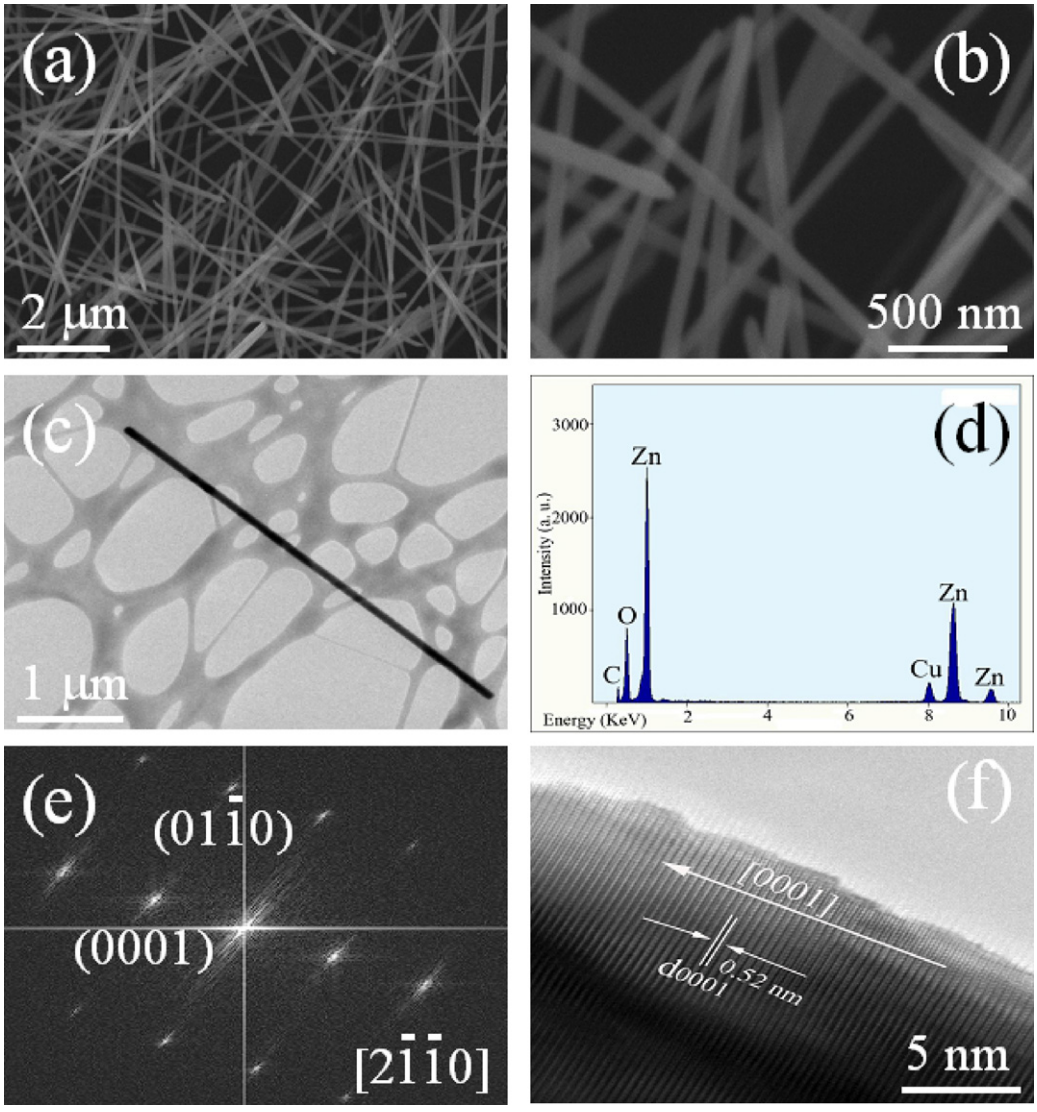

Fig. 2. (a–b) SEM and enlarged SEM images of the obtained ZnO nanowires, respectively. (c) TEM image of an individual ZnO nanowire. (d) EDS spectrum collected from the individual ZnO nanowire. (e) FFT pattern of the nanowire. (f) HRTEM image of the nanowire.

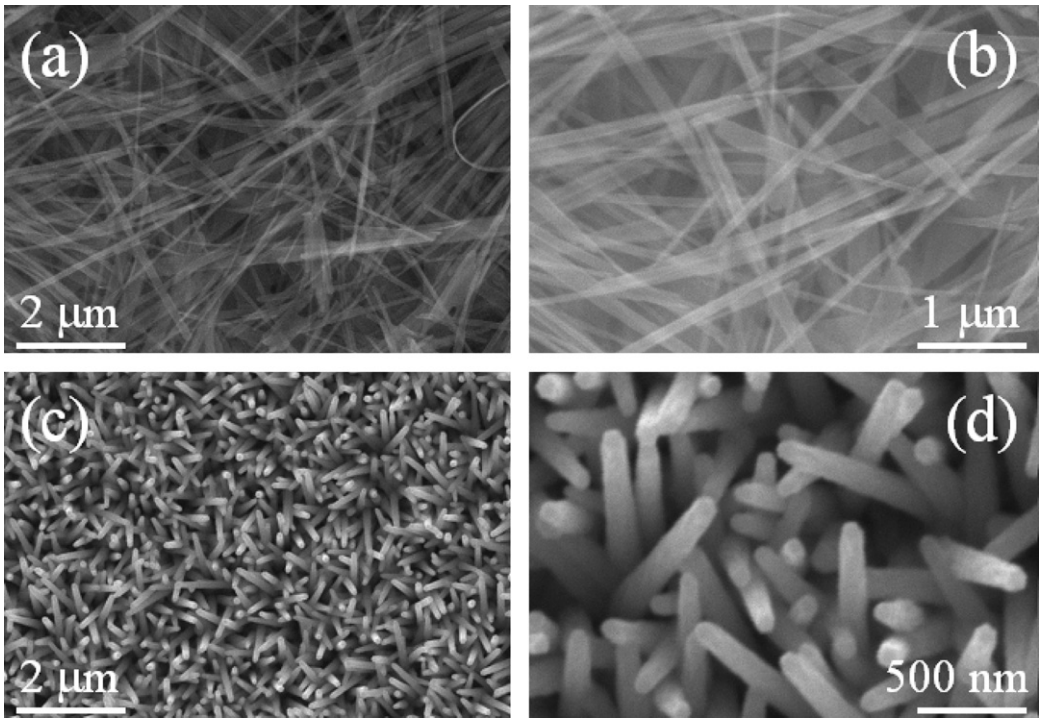

Fig. 3. (a–b) SEM and enlarged SEM images of the obtained ZnO nanobelts, respectively. (c–d) SEM and enlarged SEM images of the obtained ZnO nanorod arrays grown on 6H–SiC substrates, respectively.

enlarged SEM image of the products (Fig. 2b). The average diameter and length of these nanowires are 100 nm and 4 μm, respectively, typically shown in Fig. 2c. No rough double tips of the nanowires are observed, indicating the perfect hydrothermal growth process of the ZnO nanowires. The composition of the nanowires can be further confirmed by the TEM-based EDS measurement. As shown in Fig. 2d, the nanowire is composed of Zn and O elements, further confirming the chemical formation of ZnO. The detected C and Cu come from the Cu grid. The corresponding HRTEM image recorded along [2 $\bar{1}$ $\bar{1}$ 0] zone axis clearly shows fringe spacings of 0.52 nm, well corresponding to d_{0001} spacings of wurtzite ZnO (Fig. 2f). Based on HRTEM image of the nanowire and the fast Fourier transformation (FFT) (Fig. 2e), the nanowire is determined to grow along [0 0 0 1], and no stacking faults and dislocations are observed, revealing the well crystalline nature of the ZnO nanowire.

As shown in Fig. 1b, all the XRD diffractions peaks of the nanobelts agree well with wurtzite ZnO. The XRD pattern is similar to that of ZnO nanowires, in addition to that the intensity of the diffraction peaks was lowered. Fig. 3a–b shows the overall and enlarged SEM image of the ZnO nanobelts, respectively. It can be observed that the products are composed of predominant nanobelts and few nanowires (Fig. 3a). The length and width of nanobelts are not uniform and widths of ZnO nanobelts are in the range of 60–120 nm, as shown in Fig. 3b. Nevertheless, if the ZnO seed layer was used in the hydrothermal process, ZnO nanorod arrays can be grown on the ZnO seed layer-coated 6H–SiC substrates. Fig. 1c shows the XRD pattern of the as-deposited ZnO nanorod arrays. Only four diffraction peaks of the nanowire arrays indexed as (0 0 2), (1 0 1), (1 0 2) and (1 0 3) are observed. The overwhelming (0 0 2) peak indicates that the preferred orientation of ZnO product is along the *c*-axis and almost perpendicular to the 6H–SiC substrates, which can be further confirmed by SEM images of the products. Fig. 3c gives an on overall view of the sample revealing that there are large-scale nanorods with high density distributed over the entire surface of the substrate. These nanorods are of uniform size, and the average diameter and length are 80 nm and 1 μm, respectively, as shown in Fig. 3d. The nanorod arrays grown on special substrates e.g. SiC are of the promising applications in light-emitting diodes, laser devices, and light detectors [25].

It is reported that some capping molecules can influence the growth pattern of nanosized nuclei under non-equilibrium kinetic growth conditions in the solution-based methods [26,27]. PSMA, one of the important organic chemicals, is used in templating some nuclei and growth of alkaline-earth metals-related compounds such as $CaCO_3$ [28]. In the hydrothermal process, PSMA can interact with ZnO nuclei to form complex intermediates, and the intermediates are adsorbed on the circumference of the ZnO nuclei, resulting in the active sites generating on the surface due to the decrease of surface energy of ZnO. ZnO nanowires and nanobelts can grow on those active sites. So, PSMA is used as a spatial template for the one-dimensional growth of ZnO nuclei. Nevertheless, the detailed mechanism between PSMA and ZnO nuclei is unclear and needs to be further investigated.

Fig. 4 shows the room-temperature PL spectra of the ZnO nanostructures obtained at different experimental conditions. Though all the samples show the UV emission and green emission, the intensity ratio of the UV emission and green emission is different, indicating the diverse PL properties of the nanostructures. The intensity ratio of the UV emission and green emission observed in nanorod arrays is largest (Fig. 4c), while lowest in nanobelts (Fig. 4b). Though several different hypotheses on the origin of the green emission have been proposed and are still the subjects of considerable debates, the origin of green emission from ZnO is generally associated with intrinsic point defects such as oxygen vacancy (V_O), zinc vacancy (V_{Zn}), zinc interstitial (Zn_i), and oxygen interstitial (O_i), and/or surface defects, and related to synthesis methods [29–32]. As for the ZnO synthesized in the hydrothermal conditions, surface defects are main reason for the detected green emission [32]. As mentioned above, the organic additive PSMA offers space template for 1D growth of ZnO and are further attached on the surface of the ZnO during the secondary growth, which results in more surface defects of ZnO nanobelts. Nevertheless, assisted by the ZnO

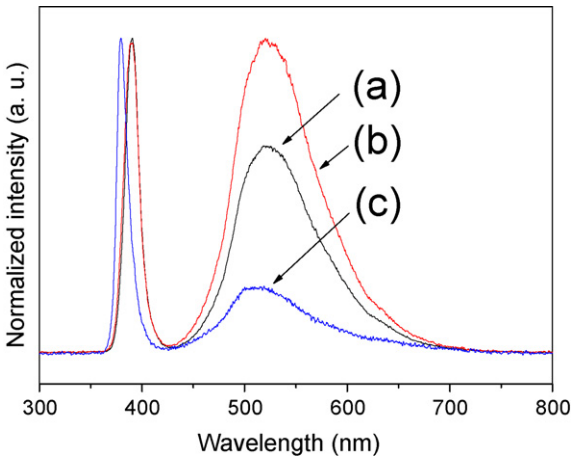

Fig. 4. Room-temperature PL spectra of the obtained ZnO nanostructures: (a) nanowires; (b) nanobelts; (c) nanorod arrays.

seed layers, the ZnO nanorod arrays began to vertically grow initiating from the ZnO seed grains via self-assembly process without PSMA. In the self-assembly process, the surface defects only originate from secondary growth and are not related to PSMA, which results in the green emission with the lowest intensity.

4. Conclusions

ZnO nanowires, nanobelts and nanorod arrays grown on 6H–SiC substrates with the same [0 0 0 1] growth direction were fabricated by a facile PSMA-assisted hydrothermal method. The nanowires are of uniform size, smooth surface and good toughness, and the average diameter and length of these nanowires are 100 nm and 4 μm, respectively. The nanobelts are not uniform in length and width, and widths of ZnO nanobelts are in the range of 60–120 nm. Highly dense nanorod arrays with uniform size and hexagonal cross-section are also fabricated on the 6H–SiC substrates. The PL measurements reveal that these nanostructures exhibit different PL properties. Though these nanostructures exhibit coexistence of UV and green emission, the strongest and weakest UV performance are observed in ZnO nanorod arrays and nanobelts. We deduce that surface defects introduced by PSMA and secondary self-assembly growth of ZnO should be responsible for the difference in PL properties of these nanostructures.

Acknowledgements

This work was supported by the National Natural Science Foundation of China (60571029, 50672088).

References

[1] J. Hu, T.W. Odom, C.M. Lieber, Acc. Chem. Res. 32 (1999) 435–445.
[2] P.G. Li, M. Lei, W.H. Tang, X. Guo, X. Wang, J. Alloys Compd. 477 (2009) 515–518.
[3] Z.W. Pan, Z.R. Dai, Z.L. Wang, Science 291 (2001) 1947–1949.
[4] P.G. Li, X. Guo, X.F. Wang, W.H. Tang, J. Alloys Compd. 479 (2009) 74–77.
[5] Y.N. Xia, P.D. Yang, Y. Sun, Y. Wu, B. Mayers, B. Gates, Y. Yin, F. Kim, H. Yan, Adv. Mater. 15 (2003) 353–389.
[6] E.M. Wong, P.C. Searson, Appl. Phys. Lett. 74 (1999) 1746–1748.
[7] E.A. Meulenkamp, J. Phys. Chem. B 102 (1998) 5566–5572.
[8] Z.M. Liao, Y. Lu, J. Xu, J.M. Zhang, D.P. Yu, Appl. Phys. A-Mater. Sci. Proc. 95 (2009) 363–366.
[9] S. Karan, B. Mallik, Nanotechnology 19 (2008) 495202.
[10] S.J. Pearton, W.T. Lim, J.S. Wright, L.C. Tien, H.S. Kim, H.T. Wang, B.S. Kang, F. Ren, J. Jun, J. Lin, A. Osinsky, J. Electr. Mater. 37 (2008) 1426–1432.
[11] P.X. Cao, Y. Ding, Z.L. Wang, Nano Lett. 9 (2009) 137–143.
[12] M.H. Huang, S. Mao, H. Feick, H.Q. Yan, Y.Y. Wu, H. Kind, E. Weber, R. Russo, P.D. Yang, Science 292 (2001) 1897–1899.
[13] Z.L. Wang, J.H. Song, Science 312 (2006) 242–246.
[14] P.G. Li, W.H. Tang, X. Wang, J. Alloys Compd. 479 (2009) 634–637.
[15] J.Y. Lao, J.G. Wen, Z.F. Ren, Nano Lett. 2 (2002) 1287–1291.
[16] P.G. Li, X. Wang, W.H. Tang, J. Alloys Compd. 476 (2009) 744–748.
[17] Y.W. Heo, V. Varadarajan, M. Kaufman, K. Kim, D.P. Norton, F. Ren, P.H. Fleming, Appl. Phys. Lett. 81 (2002) 3046–3048.
[18] Y. Li, G.W. Meng, L.D. Zhang, F. Phillipp, Appl. Phys. Lett. 76 (2000) 2011–2013.
[19] S. Yamabi, H. Imai, J. Mater. Chem. 12 (2002) 3773–3778.
[20] B. Liu, H.C. Zeng, Langmuir 20 (2004) 4196–4204.
[21] X.L. Zhang, Y.S. Kang, Inorg. Chem. 45 (2006) 4186–4190.
[22] Y. Zhou, W.B. Wu, G.D. Hu, H.T. Wu, S.G. Cui, Mater. Res. Bull. 43 (2008) 2113–2118.
[23] M. Guo, P. Diao, S.M. Cai, Appl. Surf. Sci. 249 (2005) 71–75.
[24] J.R. Carrajal, Fullprof Version 3.5, Laboratoire Leon Brillouin (CEA-CNRS).
[25] W.J. Mai, P.X. Gao, C.S. Lao, Z.L. Wang, A.K. Sood, D.L. Polla, M.B. Soprano, Chem. Phys. Lett. 460 (2008) 253–256.
[26] S.M. Lee, S.N. Cho, J. Cheon, Adv. Mater. 15 (2003) 441–444.
[27] H. Zhang, D.R. Yang, Y.J. Ji, X.Y. Ma, J. Xu, D.L. Que, J. Phys. Chem. B 18 (2004) 3955–3958.
[28] M. Lei, W.H. Tang, L.Z. Cao, P.G. Lim, J.G. Yu, J. Crystal Growth 294 (2006) 358–366.
[29] L.S. Huang, S. Wright, S.G. Yang, D.Z. Shen, B.X. Gu, Y.W. Du, J. Phys. Chem. B 108 (2004) 19901–19903.
[30] J.C. Johnson, H.Q. Yan, P.D. Yang, R.J. Saykally, J. Phys. Chem. B 107 (2003) 8816–8828.
[31] D. Stichtenoth, C. Ronning, T. Niermann, L. Wischmeier, T. Voss, C.J. Chien, P.C. Chang, J.G. Lu, Nanotechnology 18 (2007) 435701–435705.
[32] K.H. Tam, C.K. Cheung, Y.H. Leung, A.B. Djurisic, C.C. Ling, C.D. Beling, S. Fung, W.M. Kwok, W.K. Chan, D.L. Phillips, L. Ding, W.K. Ge, J. Phys. Chem. B 110 (2006) 20865–20871.